An FMRI-compatible System for Targeted Electrical Stimulation

Louise Møller Jørgensen (louisemoeller@nru.dk)
Copenhagen University Hospital: Rigshospitalet https://orcid.org/0000-0002-6084-8586
Anders Ohlhues Baandrup
Zealand University Hospital Roskilde: Sjaellands Universitetshospital Roskilde
Joseph Mandeville
Athinoula A Martinos Center for Biomedical Imaging
Andreas Nørgaard Glud
Aarhus University Hospital Skejby: Aarhus Universitetshospital
Jens Christian Hedemann Sørensen
Aarhus University Hospital Skejby: Aarhus Universitetshospital
Pia Weikop
University of Copenhagen Panum Institute: Kobenhavns Universitet Panum Instituttet
Bo Jespersen
Rigshospitalet Neurokirurgisk Klinik
Adam Espe Hansen
Rigshospitalet Klinik for Klinisk Fysiologi Nuklearmedicin og PET: Rigshospitalet Klinik for Klinisk Fysiologi Nuklearmedicin og PET
Carsten Thomsen
Zealand University Hospital Roskilde: Sjaellands Universitetshospital Roskilde
Gitte Moos Knudsen
Rigshospitalet Neurologisk Klinik

Research

Keywords: Electroceutical therapy, Deep Brain Stimulation, Optic fiber, fMRI, Radiofrequency emission, RF Noise Spectrum, pig brain

Posted Date: March 18th, 2021

DOI: https://doi.org/10.21203/rs.3.rs-313183/v1

Abstract

Background

Electroceutical therapy, applied in various forms, is a rapidly growing therapeutic option to be considered across different medical disorders, particularly within psychiatry, neurology, chronic pain and rehabilitation therapy. Combining targeted electric stimuli with feedback from fMRI can provide valuable information about the mechanisms underlying the therapeutic effects. So far, however, such studies have been hampered by the lack of technology to conduct such experiments in a both accurate and safe manner. We here present a patented system, a fMRI compatible electrical stimulator, developed for fMRI data acquisition during deep brain stimulation (DBS), as well as the first proof-of-concept neuroimaging data in pigs obtained with a prototype of the device.

Methods

The system consists of two modules, placed in the control and scanner room, with corresponding optical modules and signal converters, connected by optical fiber led through wave guides and back looped for quality assurance. The system is also connected to the MRI scanner to timely initiate the stimulation sequence at start of scan. We evaluated the system in four pigs with DBS in the subthalamic nucleus (STN) where we acquired the BOLD response in the STN and neocortex, with stimulation turned on and off in a block design synchronized to the scanning sequence.

Results

We found that the system delivered a robust electrical stimulus to the implanted electrode during the entire experimental period. The stimulus was confirmed to be in sync with the preprogrammed fMRI block design. All pigs displayed a DBS-STN induced neocortical BOLD response, but none in the site of the implanted electrode. The system solves three major problems related to electrical stimuli and fMRI examinations, namely preventing *distortion* of the fMRI signal, enabling *communication* that synchronize the experimental conditions, and surmounting the *safety hazards* caused by interference from the powerful magnetic field and RF emission.

Conclusions

The patented fMRI compatible electrical stimulator, based on an optic fiber solution, circumvents previous problems related to DBS electroceuticals and fMRI. The system allows flexible modifications for fMRI designs and stimulation parameters but can also be customized to electroceutical applications beyond DBS, applicable for a broad range of medical conditions.

Background

Electroceutical therapy is a rapidly expanding therapeutic option used across diverse medical specialties to treat patients with disorders not controlled by medicine. Single interventions with cardiac defibrillators

and electroconvulsive therapy are renowned tools, while long-term stimulations are best known in forms of cardiac pacemakers, bionic implants and replacements as well as numerous types of neurostimulators. Such devices for electrical modulation of brain function when no other effective treatments are available for brain disorders is a new frontier of medicine also known as *neuromodulation* or *neural electroceutical therapy*.

Although the therapeutic effect of electroceutical therapy is well-established for a broad range of neuropsychiatric conditions(1) and chronic pain(2), and also in, e.g., cardiac disorders, the underlying physiological mechanisms behind these treatments remain unclear. Since bioelectronic medicine target individual nerve fibers or specific brain circuits to treat a condition, a perspicuous step towards development of electroceutical therapy is to map neural circuits associated with disease, and then identify the candidate anatomical sites of intervention and transmission patterns associated with health so that these can be replicated(3). Such fingerprints can provide clinicians with a very important tool to fast track and personalize bioelectronic medicine with the potential to set optimal stimulation parameters at once, thereby saving the patients for numerous visits in the outpatient clinic for tedious adjustments and risk of proceeding therapy on suboptimal settings.

One way to achieve such insights is by combining electrical stimuli with feedback from functional magnetic resonance imaging (fMRI) to measure neural activity in terms of induced changes in cerebral blood flow and metabolism. Although such experiments are likely to make an important contribution to the understanding of how electroceuticals work in the brain, progress has been hampered by the lack of a technology to accurately conduct such experiments. Delivering an electrical stimulus to a subject during fMRI is problematic for a number of reasons. Firstly, *distortion* of the fMRI signal is imposed by emission of radiofrequency (rf) radiation from the electronic device. Secondly, proper *communication* that synchronizes the electrical stimulus with the fMRI design and initiation of the scanner sequence is needed, and thirdly, there are potential *safety hazards* can occur from interference of the powerful magnetic field with the electronic device and electrode.

The RF emission transmitted from external sources coupling into connecting cables increases noise and artefact of the obtained fMRI data signal, causing a characteristic pattern of straight lines (4). The image quality can also be disrupted by susceptibility artefacts proximate to natural interfaces or implanted hardware, which is of particular importance if the signal loss coincides with the area of expected activation.

Electroceutical therapy is generally applied in a continuous form of frequency, pulse width and voltage/amplitude, ramping at start of stimulation, and can be switched ON and OFF using a manual control unit. Accordingly, fMRI experiments have often been conducted in a block design with a ON vs OFF mode. The switching between ON and OFF states of electric stimulation in a block design requires an automated control to avoid time-delay which otherwise will disrupt the data.

There is ample level of evidence to support the safety of inactive or disconnected neurostimulators during diagnostic MRI examinations at lower strength fields (4). The hardware does not affect structural MR-

imaging, except from susceptibility artefacts close to the electrode, and it works properly when switched back on after imaging (4). However, safety concerns emerge, when the electrode is connected to an active electric stimulator switched on and off during an fMRI examination. The RF emission and fast switching gradients, such as used in fMRI sequences, can induce a voltage, which may increase the temperature in the electrode, evoke an unintended neurostimulation if the amplitude is high enough, or increase the intensity of the delivered stimulus (4). Moreover, if there are loose connections or defective leads, all energy will be deposited at site of the increased resistance, causing hazardous heating or even sparking(4).

This study describes a system that allows for delivering an adjustable electrical impulse to a subject while placed in an MR scanner, without disrupting or altering the delivered electrical signal or interfering with the obtained MRI signal.

Methods

Description of the developed system architecture

The patented system (EPS 17195244.3–1666, October 2017) consists of two modules (Fig. 1), the Main unit and the MRI unit (Fig. 1), connected by optical fiber via wave guides into the MRI scanner room. The Lead Unit is placed outside the scanner room and coupled to a computer, which enables the programming of stimulus settings and fMRI design by use of E-prime® (Psychology Software Tools, Sharpsburg, Pennsylvania, USA). Also, it is connected to the MRI scanners trigger unit which serves to timely initiate the stimulation sequence at the start of the scan. The Lead unit consists of the following: Signal generator to produce the voltage-driven electric stimulation signal; oscilloscope monitors to record the electric stimulation signal transmitted back from MRI unit for quality assurance (QA) and; and two optical modules used for transmitting the electric stimulation signal and QA signals to and from the MRI unit. The MRI unit has two corresponding optical modules and optical signal converters. The electronics in the MRI scanner room are shielded by use of caging and cable traps.

The system works as follows: When the MRI scanning is initiated, the Control unit receives an input trigger signal from the MRI scanner which initiate the pre-programmed stimulation sequence (fMRI design) and settings (volt, pulse width and frequency). The Lead unit converts the electric stimulus to an optical signal that is transmitted through wave guides to the MRI unit inside the scanner room. Here, the optical signal is converted back to an electric stimulus, which is then looped back to the Lead unit for QA before transmission of the electric stimulus to the implanted electrode in the pig brain during scan.

System adversity test (dry runs)

Image quality

To ensure that our device does not generate RF noise, which could cause image artefacts, we employed the RF Noise Spectrum sequence, which can be utilized to locate the source of an external RF

interference. The RF Noise Spectrum sequence is comparable to that of the TIM TRIO sequence for RF noise and spike check developed by The Martinos Center for Biological Imaging and involving Massachusetts General Hospital, Harvard and Siemens, as detailed in http://cbs.unix.fas.harvard.edu/science/core-facilities/neuroimaging/facilities/noise_spike.

The RF Noise spectrum sequence does not use any RF transmitter or gradient pulses, but performs simply by opening the MRI receiver during scan. The sequence runs for 30 seconds and makes 50 measurements in 10KHz frequency ranges around the central frequency of the scanner [0 ± 500 KHz], creating a noise summary image of the mean signal intensity of all the frequency bands. The results are showed as a graphical display in the patient browser, or it can be viewed in real time via the inline display. RF noise is detected as sizeable spikes of the particular frequency band in sight.

We conducted noise scans with our stimulator connected to DBS electrodes placed in a phantom, in the following conditions: a) Stimulation ON, b) Stimulation OFF, c) Alternating stimulation ON (15 sec) vs OFF (15 sec), d) Noise *(doors open)*, and e) Control *(no device in the scanner room)*. To eliminate other potential sources for external RF emission, we also ran the test without the coil placed on the electrodes, and with lights turned both on and off during scan.

All conditions were compared to control by visual inspection for spikes and dissimilarities in the RF Noise on the graphical display, but also in the active measurement output given as the maximum single measurements as well as the average mean of all 30 measurements.

Time accuracy, signal stability and functionality of the device

For quality assurance, we designed the device with a back-loop and logging of the electric signal delivered to the electrode to ensure time-accuracy and constancy of stimulation parameters following the signal conversions in the MRI environment. The back-looped signal was displayed on two systems. First, an oscilloscope was used to monitor amplitude, frequency and pulse width of the back-looped electric stimulus. Moreover, we also monitored the back-looped signal using a color-coded screen of green (stimulation ON) and black (stimulation OFF) and used a time-clock to test that the duration of the blocks (ON and OFF) was in accordance with the preprogrammed fMRI paradigm. Finally, we monitored the functioning of the device for unintentional stops during scan, such as reported in previously DBS-fMRI studies(4) using cables led via waveguides.

Animals, housing and anesthesia

All animal experiments were performed in accordance with the European Communities Council Resolves of 22 September 2010 (2010/63/EU) and approved by the Danish Veterinary and Food Administration's Council for Animal Experimentation (Journal No.1012-15-2934-00156), and is in compliance with the ARRIVE guidelines (www.nc3rs.org.uk/arrive-guidelines).

In this study, we used four female 9-10-week old pigs (crossbred Landrace, Yorkshire and Duroc, acquired from an agricultural herd) weighing 21 ± 1.5 kg (mean ± SD). After arrival to the Department of Experimental Medicine at the University of Copenhagen, the animals were inspected by a veterinarian and allowed to acclimatize for 1 week. The pigs were housed in groups in adjacent pens (3.8–5.4 m2) with 45–70% humidity, 19–23°C air ventilation, cyclical light (12 h), straw bedding and environment enrichment, in terms of various toys. The animals had free access to tap water, were fed a restricted diet twice a day and fasted 16 h before inducing anesthesia on the experimental day.

On the experimental day, fasting animals were premedicated by intramuscular (i.m.) injection of 0.14 mL/kg Zoletil® 50 Vet (Virbac, Kolding, Denmark) mixture with 6.25 Pt. xylazine (20 mg/mL) + 1.25 Pt. ketamine (100 mg/mL) + 2 Pt. butorphanol (10 mg/mL) + 2 Pt. methadone (10 mg/mL), weighed and intubated. Anesthesia was induced with 0.5-1 mL intravenous bolus injections of 10 mg/ml propofol (Fresenius Kabi AS, Halden, Norway), while maintaining spontaneous breathing during installation of catheters. Each animal had installed a bladder catheter, a peripheral venous catheter in both ears, one percutaneous femoral artery catheter (Arrow International Inc, Reading, PA, USA) and a small incision catheter in both mamillary veins. All incisions were preceded by local anesthesia given as a subcutaneous injection of 10 mL mixture; 1 Pt. 10 mg/ml xylocaine (AstraZeneca A/S, Copenhagen, Denmark) + 1 Pt. 5 mg/ml Bupivacain (Amgros I/S, Copenhagen, Denmark).

After a short trolley walk to the scanner facilities, the animals were connected to a ventilator with 34% O_2 and anesthesia was maintained with 1.5–2.5% isoflurane (Scanvet Animal Health A/S, Fredensborg, Denmark) on all fMRI experimental days. On other non-fMRI experimental days, standard anesthetic was infusion with propofol 15 mg/kg/h. The animal was set up with a slow dripping infusion with isotone saline and monitored throughout by visual inspection, blink reflexes, blood pressure, heart rate, respiratory frequency, capnography, oxygen saturation and temperature.

Surgical planning and surgery

An MR compatible stereotaxic system for pigs (NeuroLogic, Aarhus, Denmark) was used for targeting and implantation of the DBS electrodes and microdialysis probes. The system is comprised of a stereotaxic localizer box with 1) two MRI compatible detachable side plates containing a copper sulfate fiducial marking system that defines a Leksel stereotaxic space, and 2) one detachable arch-based frame for isocentric stereotaxy with a lead implantation device (LID) attached to the arch (5,6).

With the pig placed in prone position and the head fixed in the stereotaxic localizer box attached with the fiducial side plates and an adapted radiofrequency coil, structural T1/T2 MR images (Siemens 3 Tesla mMR hybrid PET-MR scanner) were obtained in each animal to visualize the fiducial markings and the subcortical target(7), followed by manual calculation, using Brain Lab®(BrainLAB AG, Germany), of the stereotaxic coordinates for targets sites and trajectories to the STN.

Next, the fiducial side plates were replaced with the arch-based frame followed by exposure of the sagittal and coronal sutures by a midline incision. Bilateral burr holes to the dura were made to target the medial

prefrontal cortex (mPFC) according to a previously validated paradigm (8) and to the MRI guided stereotaxic entry point coordinates to the STN. Next, the guide tube with a blunt cannula was inserted to a location 5 mm above the target coordinate of the STN, where the blunt cannula was removed. The quadripolar (contacts labelled 0, 1, 2, and 3) DBS electrode with internal stylet (Model 3389, Medtronic Inc., Minneapolis, MN, USA) was inserted through the guide tube and gently advanced to the target and stabilized with a two-component surgical adhesive (BioGlue, Cryolife International Inc., Kennesaw, GA, USA) before retracting the stylet and guide tube (9–11). The electrode was fixed with BioGlue to the skull and a frontally placed anchor screw, and the procedure was repeated on the contralateral side. Finally, the incision was sutured and the stereotaxic frame detached from the animal, leaving the electrodes externalized.

The animal was returned to the scanner and placed in the prone position, and the DBS electrodes were connected to the fMRI compatible electrical stimulator with cables and electrodes placed in the z-direction of the PET/MRI scanner.

Before continuing the experiments, preliminary confirmation of the correct position of the electrodes was confirmed by a postsurgical structural T1/T2 MRI scan.

Structural Magnetic Resonance Images

The MR images were generated from a 3T mMR Biograph (Siemens AG, München, Germany) whole-body scanner with a radiofrequency coil (four channels, receive-only, phased array coil) adapted to the pig head. Pre -and postoperative structural T1 and T2 weighted MRI scans were obtained for targeting and implantation of the DBS electrode and alignment of the fMRI scans during data processing and analysis. The postoperative MRI served as preliminary confirmation of the electrode placed in the cerebral target before proceeding with the experimental scans.

The protocol of the T1-wighted 3D magnetic MP-RAGE MRI was: frequency direction (FD), A > > P; slice number,240, field of view (FOV), 250 mm; slice thickness (ST), 1 mm; repetition time (TR), 1900 ms; echo time (TE), 2.44 ms; inversion time (TI), 900 ms; flip angle, 9°; base resolution, 256; acquisition time (AT), 5.04 min.

The protocol of the T2-wighted 3D magnetic fast spin echo (FSE) MRI was: FD, A > > P; slice number, 240, FOV, 250 mm; ST, 1.00 mm; TR, 3200 ms; TE, 409 ms; base resolution, 256; AT, 6:26 min

Stimulation parameters, fMRI design and BOLD protocol

The frequency, pulse width and voltage were set at 125 Hz, 500 or 200 us, and 3 V (voltage) in a rectangular shape delivered between two electrode levels (0–1) of the quadripolar Medtronic 3389 electrode (Medtronics Inc).

The fMRI paradigm was a classic block design, with stimulation turned on and off in a total of 5 cycles. After two volumes of discarded acquisitions to allow for scanner equilibrium, 60 volumes of initial scanning at rest (120 seconds) were performed followed by five stimulus/rest blocks. These blocks each

consisted of 3 volumes (6 seconds) of electric stimulus (DBS-ON) and 60 volumes (120 seconds) of rest (DBS-OFF) for a total 375 volumes.

The parameters of the gradient-echo, echo-planar imaging sequence sensitive to the blood-oxygen-level-dependent (BOLD) response were: FD, A > > P; slice number, 42, FOV, 192 mm; ST, 3.00 mm; TR, 2150 ms; TE, 26 ms; flip angle, 78°, base resolution, 64; spatial resolution 3x3x3 mm, AT, 12:07 min

Euthanasia and post-mortem handling

After the final scan, the pigs were euthanized immediately with an overdose of sodium pentobarbital (ScanVet Animal Health A/S, Fredensborg, Denmark) and moved for a post-mortem CT-scan (Dual Source Somatom Definition, Siemens, Munich, Germany) of the brain before removal of the brain and electrodes(12). The CT scan was used as final validation of the correct position of the electrodes in target by co-registration to both the structural MRI and a modified pig brain atlas(13).

Data processing and analysis

After image acquisition, the time series data were processed to obtain maps of brain activation using the JIP analysis toolkit (http://www.nmr.mgh.harvard.edu/~jbm/jip/) customized with the modified pig brain atlas(13) to analyze pig fMRI data.

First, the images were pre-processed by a) Converting DICOM format to NIfTy files, b) Alignment of the structural scan to the modified pig-atlas(13), c) Motion correction (only functional scans) and correction to the hemodynamic input function d) Alignment of the functional scans to the aligned postoperative anatomical scan, and e) Register and spatial smoothing (3 mm) of all fMRI data.

Next, we determined if there was a significant activation associated with DBS-ON compared to DBS-OFF in neocortex and in STN. This was based on a generalized linear modelling (GLM) and cross-correlation with five modeled regressors that include Legendre polynomials to describe signal drift and repetitive finite-impulse response regressors to fit the hemodynamic response function. The regional or focal BOLD response was displayed in a time-dependent fashion and averaged in relation to the event across all cycles for each pig.

Results

Functionality of the device

The RF Noise Spectrum scans (Fig. 2) show that the functioning device did not produce external RF emission and spikes which interfere with the image quality. Also, we did not observe any surge lines in the images.

To illustrate what noise looks like, we added (supplementary material 1) a graphical display of a RF noise spectrum scan with doors left open during scan as compared to the other conditions with the stimulator

turned on and off, or removed from the scanner room. Moreover, we did not see any changes with lights turned on and off, or with removal of coils (not shown in supplementary material 1).

Likewise, we showed with continuous oscillatory monitoring of the back-looped signal that the stimulation parameter (voltage, pulse-width and frequency) was constant throughout the scan. Moreover, we did not experience unintentional stops of the device during any of the scans and observed an excellent time accuracy of the delivered stimulation compared to the preprogrammed paradigm.

fMRI Bold signal

With the electrode placed in target STN (Fig. 3) and the electrical signal back-looped for quality assurance, we found that the fMRI compatible stimulator delivered a robust electrical stimulus to the implanted electrode during the entire experimental period of 750 sec. The electrical stimulus was confirmed to be in sync with the preprogrammed fMRI block design, which was initiated by a trigger impulse upon start of MRI volume acquisition.

When DBS-STN was turned on, we observed a neocortical BOLD response (Fig. 4), which was reproducible across stimulation cycles and between individuals. However, no BOLD response was observed in the target site for implantation and stimulation, i.e., STN. (Fig. 4).

Discussion

We here present a patented system, a fMRI compatible electrical stimulator, as well as the first proof-of-concept neuroimaging data in pigs obtained with a prototype of the device. The system enables generation of a predefined electrical signal to be delivered to an individual while undergoing fMRI examination. Importantly, the system can synchronize the stimulation and an automated fMRI design which is triggered upon start of the first fMRI volume acquisition. The system solves three major problems related to electrical stimuli and fMRI examinations, namely preventing *distortion* of the fMRI signal, *communication* that synchronize the experimental properties, and surmounting the *safety hazards*.

Distortion

Two factors may disturb image quality, namely external RF emission and transitions in susceptibility. Like others who evaluate the effects between states of DBS during fMRI(4,14–17), we have placed the oscillating unit outside the scanner room in order to avoid problems with image quality caused by direct RF emission from the electronic device. However, this maneuver does not eliminate RF emission from external sources coupling into the connecting cables between the pulse generator and the electrodes, led through waveguides. Such external high-frequency electromagnetic power cause straight line surges across the electrode(4), and this effect cannot dependably be omitted by shielding of the cables, which add unpredictability to the examination. Our system circumvents interference from external RF sources by

converting the electric stimulus to an optic signal outside the scanner room and back to an electric stimulus inside the scanner room, easily and reliably led through waveguides.

Due to the small signal to noise ratio in GE-EPI and DTI sequences, susceptibility artefacts proximate to the electrode and lead are more prominent with fMRI than with structural imaging(18). Except in the immediate vicinity of the electrode and lead (4), the sequences are, however, still useful for data analysis. Still, this may limit the use of fMRI, particular if the susceptibility artefact occurs in the exact area of expected activation. Correspondingly, we observed a DBS-STN induced change in BOLD response in neocortex, but not in the cerebral target site for the implanted electrode and stimulation, so possible effects of DBS at stimulation site remain unknown. However, no stimulator system used in fMRI examinations, including ours, can overcome the difficulties with metallic susceptibility artefacts proximate to electrodes and leads, but future advances in carbon electrodes might(19).

Communication

It is essential to ensure that the electric stimulus is properly synchronized with the block-designed fMRI examination, including the initiation of the scanner sequence. Moreover, this communication must not be disrupted by the RF emission from the MRI scanner. To respond to these requirements, our fiber optic system, back-looped for quality assurance, prevents a) human and systemic timing errors, b) unpremeditated changes in stimulation parameters imposed on the electric stimulator by RF pulses from the MRI scanner, and c) inconsistencies in the functioning of the oscillating unit placed outside the scanner room during the experiments. The system can run numerous pre-programmed stimulation parameters and fMRI designs, which facilitate fast and simple shifts between fMRI experiments.

First, manual switch of an impulse generating (IPG) unit between the two states, ON and OFF, is too imprecise to conform to the fMRI block-design paradigms and the MR volume acquisition because the person operating an IPG unit can induce a delay. A delay can also occur between pressing the control button and until the IPG unit switches. One study demonstrates(20), that even when the IPG unit is preprogrammed to the requested change in stimulation parameters, a time delay of six seconds accumulate during an fMRI experiment. Such time-delay is enough to wobble the block-design and subsequent data analysis, particular in block-designs with short stimulation periods which typically is used with BOLD paradigms to avoid attenuation during the fMRI sequence.

A limitation with previous approaches, including ours, designed to assess changes in fMRI signal between the two states, DBS ON and OFF, is the necessity for externalized electrodes. However, one study has developed a so-called custom electronics box (20), which has the ability to decode a preprogrammed stimulation pattern outside the scanner room, and once the individual is placed in the MRI scanner, the fMRI sequence is initiated by a trigger output signal with an absolute error of 100 ms. The system allows for fMRI experiments with internalized IPG units, but the IPG unit needs to be preprogrammed and running before placing the individual in the scanner, thereby rendering the fMRI experiment susceptible to attenuation of the data signal, and it does not allow investigations of *de novo* stimulation or sequential fMRI sequences.

Moreover, even when placed outside the scanner room, RF pulses from the MRI scanner can interfere with an electric stimulator, regardless of shielding the cables between the electrode and oscillating unit. It has been shown that RF pulses can induce high voltage, which can lead to improper stimulation amplitudes or even cause the pulse generator to unintentionally switch off during examination(4). Although the stimulation unit may easily be switched back on, such flaws require constant monitoring of the apparatus and make the data acquisition prone to human errors. The Mayo Clinic (Rochester, USA) has developed a Bluetooth based communication system, WINCS(21), wherein wireless communication modules are used to communicate between inside and outside the MRI room. The WINCS system avoids direct interference from RF pulses on the electric stimulator, as there are no connecting cables led through the waveguides. One concern with the Bluetooth based system may be that the electromagnetic interference on wireless data transfer produced inside the MRI scanner imposes alterations in the delivered electrical signal. This is of particular concern to regulatory requirements in a clinical setting, when a Bluetooth based medical device is used to deliver an electroceutical therapy to an individual undergoing fMRI examination, as compared to a less critical Bluetooth function which monitors, e.g, ECG and pulse.

Safety Hazards

The possible safety issues that exist for electroceutical systems used in fMRI examinations include interaction of the magnetic field and functional disruption of the device(17). As previously mentioned, RF pulses from the MRI scanner can lead to improper stimulation or unintentional stops of the oscillating unit, even when placed outside the scanner room and shielding of connecting cables. This risk is eliminated with our stimulation system using optic fibers. Moreover, three potential mechanisms(22) caused by magnetic field interaction can induce voltage, current flow and heating in the lead and its electric circuit: 1) Electromagnetic induction heating, 2) Electromagnetic induction heating of a circuit in resonance, and 3) The antenna effect.

First, electromagnetic induction from switching gradients and RF pulses can cause: a) eddy currents to flow at the surface of any conductive material in the scanner room, b) voltage coupling into the lead with potential to increase the stimulation amplitude up to 30% with risk of even trigger unintended neurostimulation if the amplitude is high enough, or c) resistance heating when induced currents dissipate as heat occurring in locations with high resistance, such as the electrode-tissue interface. In case of disconnections or defective electrodes and leads, a sudden increase in resistance can result in excessive heating or even sparks(4). These effects can be minimized both by use of cable traps (23) and by including a feed-back to the system when output saturation or high resistance is reached. The latter is measured by an impedance-meter. Although our system does not prevent RF emission from the MRI scanner to couple into the cable leading from the electrode to the MRI unit placed outside the 200-gauss line, the systems' cables are shorter and does not extend outside the scanner room, which would add risk of picking up external RF emission.

Second, resonance heating occurs in the unlikely event when a conducting loop arranged perpendicular to the RF field magnetic field resonates at a frequency equal to that of the RF field, which increases the ability of the loop to concentrate current leading to excessive heating(2,24). Heating from large diameter

loops can be avoided by placing the lead straight in the z-direction, in the center of the magnetic core and preventing direct contact between the cables and the individual undergoing fMRI examination.

Thirdly, the antenna effect occurs when the electric component of the RF emission, rather than the magnetic component, couples into a lead equal to half the length of the RF fields wavelength or multiples hereof, thereby producing a resonant standing wave with a maximum antinodal current and heating at the open end of the lead(4). This effect can be eliminated by avoiding resonant lengths of cables.

Potential use of the system

fMRI is perfectly suited to investigate changes between states in electroceutical therapies, because the stimulation is steady, well-regulated and with reproduceable clinical effects, ideally suitable for fMRI block designs(17).

fMRI can map changes in brain activity reflecting the underlying changes in regional brain metabolism. The combination of fMRI and electroceutical therapy can provide an important tool to investigate underlying mechanisms associated with the effect of DBS, optimize the stimulation parameters coupled to a certain fMRI signal that reflects DBS clinical efficacy, and possibly distinguish responders and non-responders to therapeutic interventions. fMRI brain imaging of the effects of electrical stimuli in brain disorders where DBS is considered helpful can potentially provide the clinician with an important tool to improve therapy and potentially commence fast track and personalized medicine by prompt calibration of optimal stimulation settings, as compared to many hospital visits for tedious adjustments.

Our system has a current controlled voltage source with flexible frequency and pulse width settings appropriate for deep brain stimulation, but can be moderated to applications using a current controlled current source or higher stimulation parameters appropriate for surface electrode stimulations. The system can apply electrical stimulation equivalent to implantable and external neurostimulators used to treat neuropsychiatric disorders, rehabilitation and chronic pain therapy, and may also be modified to new applications for electroceutical therapy within ophthalmology, otology, gastroenterology, urology, cardiology, and bionic replacements.

Limitations

As previously discussed, it is difficult to assess if a fMRI signal in the stimulation target site is a real or observation or due to susceptibility artefacts from the implanted electrode (Fig. 3). Future technological advances, such as carbon electrodes, may resolve the issue.

The present prototype does not encompass an impedance-meter and a safety default system for immediate stimulation stop, but this will be included in our next generation prototype as an important safety precaution for clinical studies.

Finally, the system necessitates the electrodes to be externalized, which means that measurements can only be done in connection with the implantation or when the battery needs to be exchanged.

Alternatively, indwelling models of chronic stimulation in animal models can be accomplished by encapsulating the externalized probe contacts within headset chambers(25).

Conclusions

The presented fMRI compatible electrical stimulator delivers a predefined electrical stimulus during fMRI examination, synchronized with the fMRI design and triggered upon initiation of the fMRI sequence. The system, based on an optic fiber solution, circumvents previous problems related to DBS and fMRI, namely image distortion, improper communication and safety hazards. The system can be modified to elicit stimuli either voltage- or current-control and in addition, flexible stimulation parameters costumed to numerous electroceutical applications used within a broad range of medical conditions can be tuned. We anticipate that the system will be useful for DBS, spinal cord stimulation, cranial nerve stimulation, peripheral nerve stimulation, cortical multi-electrode stimulation, bionic replacements, cardiac pacemakers, retinal and corneal electric stimulation, cochlear implants, as well as surface-electrode stimulation in forms of auricular vagal nerve stimulation, neuromuscular electrical stimulation and transcutaneous nerve stimulation.

Abbreviations

BOLD Blood-oxygen-level-dependent

DBS Deep Brain Stimulation

fMRI Functional Magnetic Resonance Imaging

mPFC Medial prefrontal cortex

QA Quality assurance

RF Radiofrequency

STN Subthalamic nucleus

Declarations

Ethics approval

All animal experiments were performed in accordance with the European Communities Council Resolves of 22 September 2010 (2010/63/EU) and approved by the Danish Veterinary and Food Administration's Council for Animal Experimentation (Journal No.1012-15-2934-00156), and is in compliance with the ARRIVE guidelines (www.nc3rs.org.uk/arrive-guidelines).

Consent for publication

Not applicable

Availability of data and materials

The data are available from the corresponding author on reasonable request

Competing interests

The University of Copenhagen, Copenhagen University Hospital - Rigshospitalet and Copenhagen University Hospital - Roskilde have in collaboration filed an international patent application entitled System for electrical stimulation during functional MRI published as WO 2019/068884 A1 with Anders Ohlhues Baandrup, Louise Møller Jørgensen and Carsten Thomsen as the inventors. Thus, the institution and inventors have a financial interest in the patency and its developments.

The other authors declare that they have no competing interests

Funding

Funding was provided from Independent Research Fund Denmark [9039-00314B] with salary (Louise Møller Jørgensen) as well as Lundbeck Foundation [R183-2014-3836] and Novo Nordisk Fonden (0057806) for running costs. The study design, collection, analysis and interpretation of data, writing of the paper and in the decision to submit the paper for publication were not influenced by any of the funds supporting the study. The corresponding author had full access to all the data in the study and had the final responsibility for the decision to submit the data for publication.

Authors Contributions

All authors fulfill the criteria for authorship and appear on the author list. All authors revised and gave final approval of the manuscript. Following authors contributed to the conception (LMJ, AO, CT), drafting of the article (LMJ and GMK), design (LMJ, AO, CT, JHCS, AEH, BJ and GMK), acquisition of data (LMJ, AO, ANG, JHCS, PW, BJ, PW, AEH and CT), and analysis and interpretation of data (LMJ, AO, JM, AEH, CT and GMK).

Acknowledgements

We would like to thank Karen Kettless, Siemens Healthineers, Ballerup, Denmark, for assistance related to the RF Noise Spectrum sequence.

References

1. Holtzheimer PE, Mayberg HS. Deep Brain Stimulation for Psychiatric Disorders. Annu Rev Neurosci. 2011;34(1):289–307.
2. Moisset X, Lanteri-Minet M, Fontaine D. Neurostimulation methods in the treatment of chronic pain. J Neural Transm. 2020 Apr 1;127(4):673–86.
3. Famm K, Litt B, Tracey KJ, Boyden ES, Slaoui M. A jump-start for electroceuticals. Nature. 2013 Apr;496(7444):159–61.
4. Georgi J-C, Stippich C, Tronnier VM, Heiland S. Active deep brain stimulation during MRI: A feasibility study. Magn Reson Med. 2004;51(2):380–8.
5. Bjarkam CR, Cancian G, Larsen M, Rosendahl F, Ettrup KS, Zeidler D, et al. A MRI-compatible stereotaxic localizer box enables high-precision stereotaxic procedures in pigs. J Neurosci Methods. 2004 Oct 30;139(2):293–8.
6. Bjarkam CR, Cancian G, Glud AN, Ettrup KS, Jørgensen RL, Sørensen J-C. MRI-guided stereotaxic targeting in pigs based on a stereotaxic localizer box fitted with an isocentric frame and use of SurgiPlan computer-planning software. J Neurosci Methods. 2009 Oct 15;183(2):119–26.
7. Bjarkam CR, Glud AN, Orlowski D, Sørensen JCH, Palomero-Gallagher N. The telencephalon of the Göttingen minipig, cytoarchitecture and cortical surface anatomy. Brain Struct Funct. 2017 Jul 1;222(5):2093–114.
8. Jørgensen LM, Weikop P, Villadsen J, Visnapuu T, Ettrup A, Hansen HD, et al. Cerebral 5-HT release correlates with [11C]Cimbi36 PET measures of 5-HT2A receptor occupancy in the pig brain. J Cereb Blood Flow Metab. 2017 Feb 1;37(2):425–34.
9. Bjarkam CR, Jorgensen RL, Jensen KN, Sunde NAa, Sørensen J-CH. Deep brain stimulation electrode anchoring using BioGlue®, a protective electrode covering, and a titanium microplate. J Neurosci Methods. 2008 Feb;168(1):151–5.
10. Ettrup KS, Tornøe J, Sørensen JC, Bjarkam CR. A surgical device for minimally invasive implantation of experimental deep brain stimulation leads in large research animals. J Neurosci Methods. 2011 Aug 30;200(1):41–6.
11. Orlowski D, Michalis A, Glud AN, Korshøj AR, Fitting LM, Mikkelsen TW, et al. Brain Tissue Reaction to Deep Brain Stimulation—A Longitudinal Study of DBS in the Goettingen Minipig. Neuromodulation Technol Neural Interface. 2017;20(5):417–23.
12. Bjarkam CR, Orlowski D, Tvilling L, Bech J, Glud AN, Sørensen J-CH. Exposure of the Pig CNS for Histological Analysis: A Manual for Decapitation, Skull Opening, and Brain Removal. J Vis Exp JoVE. 2017 13;(122).
13. Villadsen J, Hansen HD, Jørgensen LM, Keller SH, Andersen FL, Petersen IN, et al. Automatic delineation of brain regions on MRI and PET images from the pig. J Neurosci Methods. 2018 Jan 15;294(Supplement C):51–8.

14. Phillips MD, Baker KB, Lowe MJ, Tkach JA, Cooper SE, Kopell BH, et al. Parkinson Disease: Pattern of Functional MR Imaging Activation during Deep Brain Stimulation of Subthalamic Nucleus—Initial Experience. Radiology. 2006 Apr 1;239(1):209–16.
15. Stefurak T, Mikulis D, Mayberg H, Lang AE, Hevenor S, Pahapill P, et al. Deep brain stimulation for Parkinson's disease dissociates mood and motor circuits: A functional MRI case study. Mov Disord. 2003 Dec 1;18(12):1508–16.
16. Arantes PR, Cardoso EF, Barreiros MÂ, Teixeira MJ, Gonçalves MR, Barbosa ER, et al. Performing functional magnetic resonance imaging in patients with Parkinson's disease treated with deep brain stimulation. Mov Disord. 2006;21(8):1154–62.
17. Rezai AR, Lozano AM, Crawley AP, Joy MLG, Davis KD, Kwan CL, et al. Thalamic stimulation and functional magnetic resonance imaging: localization of cortical and subcortical activation with implanted electrodes: Technical note. J Neurosurg. 1999 Mar 1;90(3):583–90.
18. Boutet A, Rashid T, Hancu I, Elias GJB, Gramer RM, Germann J, et al. Functional MRI Safety and Artifacts during Deep Brain Stimulation: Experience in 102 Patients. Radiology. 2019 Aug 6;293(1):174–83.
19. Zhao S, Li G, Tong C, Chen W, Wang P, Dai J, et al. Full activation pattern mapping by simultaneous deep brain stimulation and fMRI with graphene fiber electrodes. Nat Commun. 2020 Apr 14;11(1):1788.
20. Fiveland E, Madhavan R, Prusik J, Linton R, Dimarzio M, Ashe J, et al. EKG-based detection of deep brain stimulation in fMRI studies. Magn Reson Med. 2018;79(4):2432–9.
21. Bledsoe JM, Kimble CJ, Covey DP, Blaha CD, Agnesi F, Mohseni P, et al. Development of the Wireless Instantaneous Neurotransmitter Concentration System for intraoperative neurochemical monitoring using fast-scan cyclic voltammetry. J Neurosurg. 2009 Oct;111(4):712–23.
22. Dempsey MF, Condon B, Hadley DM. Investigation of the factors responsible for burns during MRI. J Magn Reson Imaging. 2001;13(4):627–31.
23. Seeber DA, Jevtic J, Menon A. Floating shield current suppression trap. Concepts Magn Reson Part B Magn Reson Eng. 2004;21B(1):26–31.
24. Bennett MC, Wiant DB, Gersh JA, Dolesh W, Ding X, Best RCM, et al. Mechanisms and prevention of thermal injury from gamma radiosurgery headframes during 3T MR imaging. J Appl Clin Med Phys. 2012 Jul;13(4):54–70.
25. Arsenault JT, Vanduffel W. Ventral midbrain stimulation induces perceptual learning and cortical plasticity in primates. Nat Commun. 2019 Aug 9;10(1):3591.

Figures

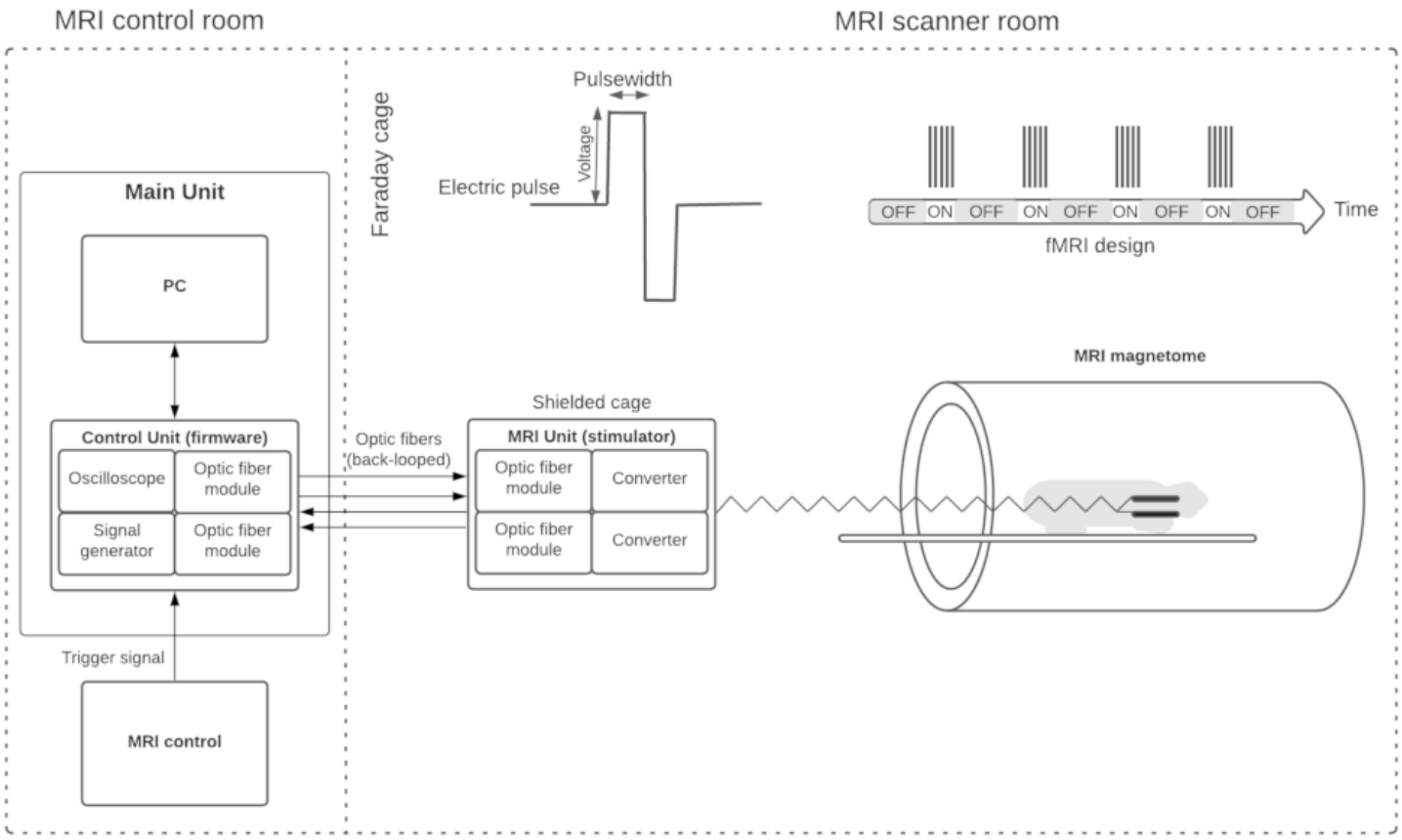

Figure 1

Diagram of the fMRI-compatible system architecture The system consists of two units, the Control unit and the MRI unit (stimulator), placed outside and inside the MRI scanner room respectively. The units communicate through optical fibers led through wave guides between the scanner room and control room.

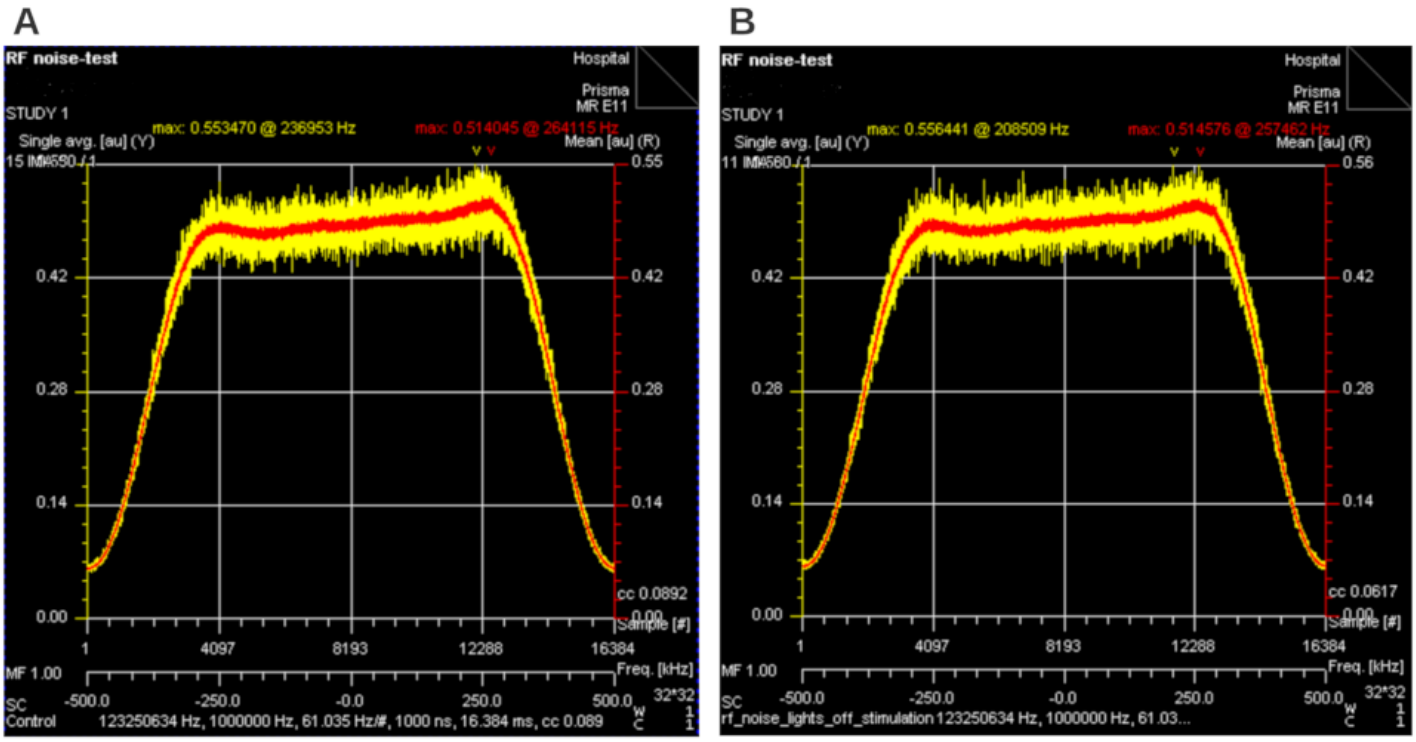

Figure 2

Graphical display of the RF noise spectrum The signal intensity of each RF noise scan is displayed as individual rows of all frequency band ±500 KHz to the central scanner frequency in the column directions. Yellow indicates the single active measurements, and red indicates the averaged mean signal of 30 measurements. There are no dissimilarities in the RF noise spectrum with the stimulator ON (right) as compared to control (left), where the device was not present in the scanner room.

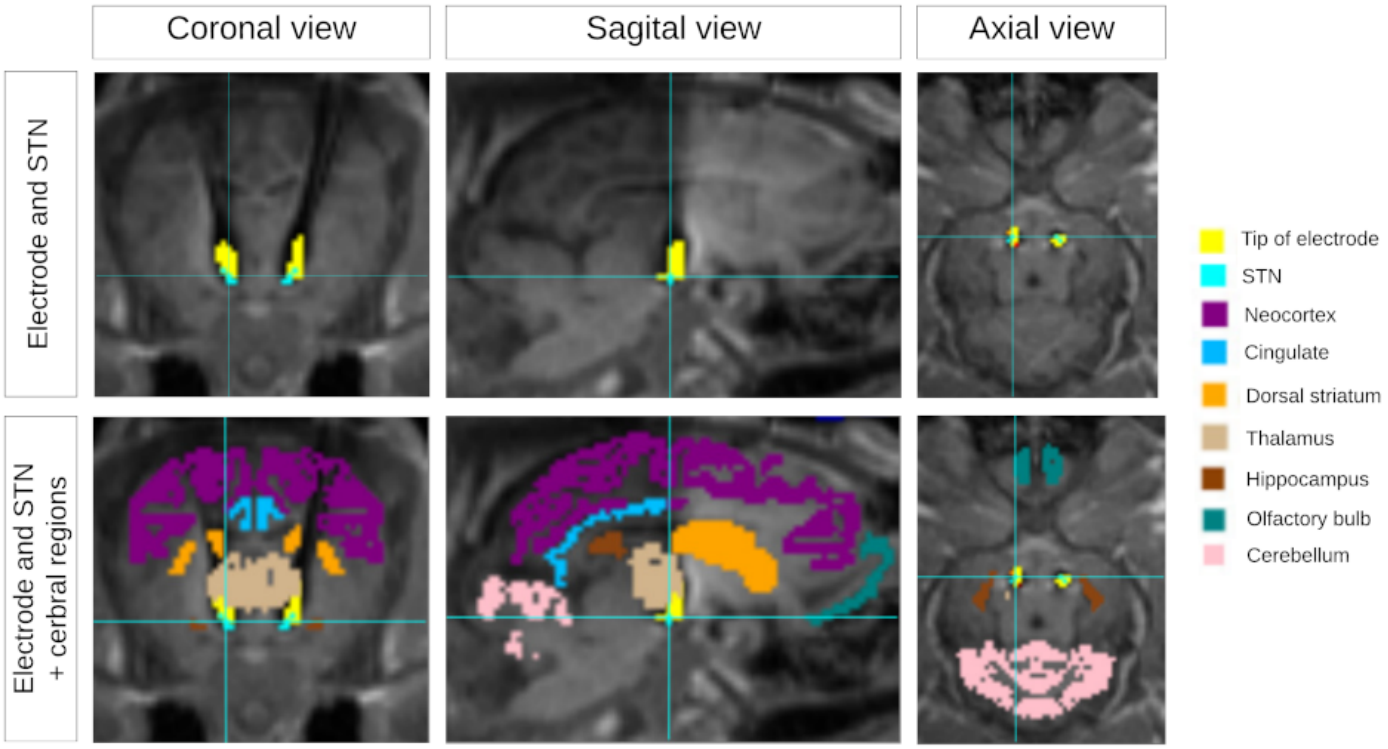

Figure 3

Electrode placement in STN The top panel shows the placement of the tip of the electrode (yellow) relative to the DBS target in STN (blue-green). The bottom panel display an overlay of additional cerebral regions. The figure is an overlay of the postoperative MRI scan of the pig brain are co-registered to both the modified pig-atlas (regional overlays) and a postoperative CT scan (electrode). All the images show signal loss caused by susceptibility artefacts proximate to the electrode. The cross shows the coordinate in right STN for the three views.

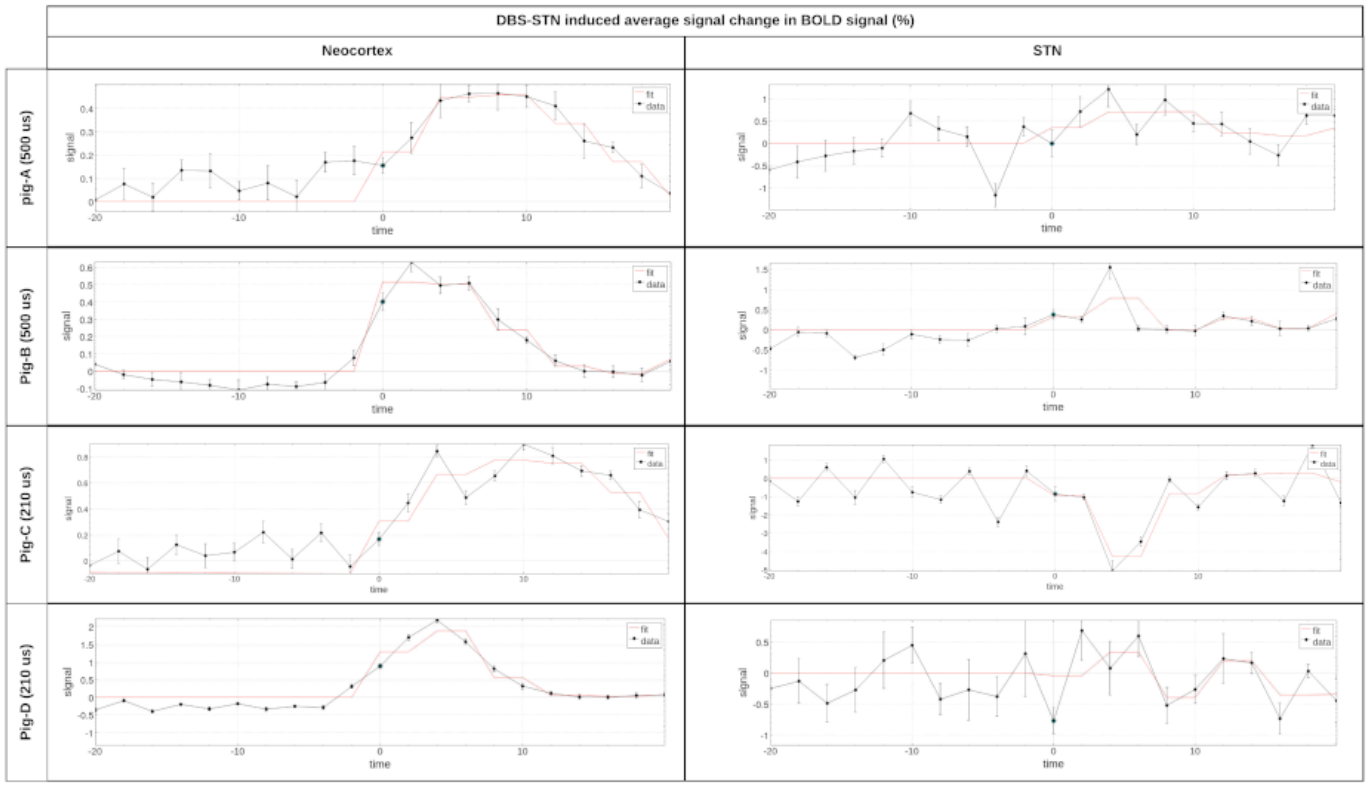

Figure 4

BOLD signal in neocortex and STN following DBS-STN The DBS-STN induced fMRI response in four pigs (rows) are displayed for two cerebral regions, neocortex (left column) and STN (right column). The average BOLD signal changes across five cycles of DBS-STN with stimulation settings 130 Hz, 3V and either 210 us (n=2) and 500 us (n=2). Time 0 indicates start of the stimulation period. The data (black) is given as the average percentual BOLD signal change ± SD for each pig, as well as the fitted data to the model (red).

Supplementary Files

This is a list of supplementary files associated with this preprint. Click to download.

- Supplementarymaterial1.docx